Geophysical Journal International

Geophys. J. Int. (2013) **195,** 544–557
Advance Access publication 2013 July 18

doi: 10.1093/gji/ggt241

Attenuation character of seismic waves in Sikkim Himalaya

Pinki Hazarika,[1] M. Ravi Kumar[1] and Dinesh Kumar[2]

[1]*National Geophysical Research Institute (CSIR), Uppal Road, Hyderabad* 500 007, *India. E-mail: pinkihazarika14@gmail.com*
[2]*Kurukshetra University, Kurukshetra, Haryana, India*

Accepted 2013 June 17. Received 2013 April 18; in original form 2012 May 16

SUMMARY

In this study, we investigate the seismic wave attenuation beneath Sikkim Himalaya using *P*, *S* and coda waves from 68 local earthquakes registered by eight broad-band stations of the SIKKIM network. The attenuation quality factor (Q) depends on frequency as well as lapse time and depth. The value of Q varies from (i) 141 to 639 for *P* waves, (ii) 143 to 1108 for *S* waves and (iii) 274 to 1678 for coda waves, at central frequencies of 1.5 Hz and 9 Hz, respectively. The relations that govern the attenuation versus frequency dependence are $Q_\alpha = (96 \pm 0.9) f^{(0.94 \pm 0.01)}$, $Q_\beta = (100 \pm 1.4) f^{(1.16 \pm 0.01)}$ and $Q_c = (189 \pm 1.5) f^{(1.2 \pm 0.01)}$ for *P*, *S* and coda waves, respectively. The ratio between Q_β and Q_α is larger than unity, implying larger attenuation of *P* compared to *S* waves. Also, the values of Q_c are higher than Q_β. Estimation of the relative contribution of intrinsic (Q_i) and scattering (Q_s) attenuation reveals that the former mechanism is dominant in Sikkim Himalaya. We note that the estimates of Q_c lie in between Q_i and Q_s and are very close to Q_i at lower frequencies. This is in agreement with the theoretical and laboratory experiments. The strong frequency and depth dependence of the attenuation quality factor suggests a highly heterogeneous crust in the Sikkim Himalaya. Also, the high Q values estimated for this region compared to the other segments of Himalaya can be reconciled in terms of moderate seismic activity, unlike rest of the Himalaya, which is seismically more active.

Key words: Body waves; Coda waves; Seismic attenuation; Continental margins: convergent.

GJI Seismology

1 INTRODUCTION

Attenuation of seismic waves is an ubiquitous property of the Earth, whose variation is governed by the nature of the propagation medium. The decay of energy is largely attributed to geometrical spreading, intrinsic attenuation due to inelastic nature of rocks and scattering attenuation due to inhomogeneities in the medium (Aki & Chouet 1975). Intrinsic attenuation converts the seismic energy to heat due to anelastic absorption and scattering attenuation redistributes the energy through random heterogeneities present in the upper earth medium. In a geological perspective, the Earth's lithosphere is heterogeneous owing to tectonic activities like folding, faulting and large-scale crustal movements associated with plate tectonics (Sato & Fehler 1998). Therefore, investigating the attenuation character of seismic waves in the lithosphere is important for understanding the regional earth structure and seismotectonic activity. The attenuation property is described by a dimensionless quantity called the quality factor Q, which expresses the decay of wave amplitude during its propagation in the medium (Knopoff 1964). Large values of Q imply small attenuation and vice versa. Tectonically active regions generally have a relatively high heat flow and are more attenuating than colder regions that are tectonically less active or inactive. Also, it has been observed that variations in Q values correlate with traveltime variations, with fast traveltimes typically associated with high Q and vice versa (Lay & Wallace 1995). In general, the Q value increases with frequency (Mitchell 1981) through the relation $Q = Q_0 f^n$, where 'Q_0' is the quality factor at a frequency of 1 Hz. The parameter 'n' is a measure of frequency dependence. Its value is generally close to 1 but varies from region to region, depending on the heterogeneity of the medium (Aki 1981). Globally, numerous studies have been conducted to decipher the attenuation characteristics through estimation of the quality factor Q, primarily using *P* waves (Q_α), *S* waves (Q_β), coda waves (Q_c) and *Lg* waves (Q_{Lg}; e.g. Yoshimoto *et al.* 1993; Chung & Lee 2003; Kim *et al.* 2004; Ma'hood & Hamzehloo 2009).

To gain insights into the physical mechanisms governing the attenuation properties beneath a region, it is important to separate the contributions from intrinsic (Q_i) and scattering (Q_s) attenuation. According to the thermal diffusion model for intrinsic attenuation (Zener 1948; Savage 1965, 1966; Leary 1995), when a seismic wave propagates through a crustal rock, significant dissipation of energy occurs due to heat, owing to the presence of small-scale irregularities and discontinuities such as grains, microfractures and cracks, leading to structural weakening of the crust. The magnitude and particularly the frequency dependence of this heat dissipation are strongly associated with the sizes of irregularities and

discontinuities. In addition, characterization of Q_s, specifically with regard to the magnitude of attenuation, its frequency dependence and relative contribution of scattering attenuation to total attenuation, particularly at frequencies lower than 1 Hz, is also important. Q_s plays a key role in resolving the conjecture concerned with the shape of the *S*-wave attenuation versus frequency curve (Aki 1980). From the frequency dependency of Q_s, the strength and the average size of heterogeneities in the shallow crust can be inferred, including the strongly fractured earthquake swarm regions (Matsunami & Nakamura 2004). According to Tsujiura (1978) and Aki (1980), scattering attenuation plays a more significant role than intrinsic attenuation. On the contrary, Frankel & Wennerberg (1987) proposed that intrinsic attenuation is more dominant compared to scattering attenuation. There are various examples in literature that support both the view points. The methods that are in vogue to estimate the relative contribution of Q_i and Q_s utilize the decay of total *S*-wave energy with respect to the hypocentral distance (Wu 1985), the energy flux model of coda waves based on the coda amplitude and decay (Frankel & Wennerberg 1987) and the total attenuation (Wennerberg 1993). The main objective of this study is to quantify the attenuation mechanism of Sikkim Himalaya, using the *P*, *S* and coda portions of the local earthquake seismograms and isolate the intrinsic and scattering attenuation in the eastern part of the tectonically active Himalayan orogen. Though Sikkim is situated in an active tectonic region like the Himalaya, it has only experienced moderate seismicity in the past. The region is close to the epicentre of the great 1934 Bihar–Nepal earthquake. In view of the sparse nature of seismic networks in the region the attenuation characteristics of the Sikkim Himalaya have been hitherto not studied. With the primary objective of investigating the lithospheric structure and seismicity in the region, the National Geophysical Research Institute has established a seismic network in the region. Broad-band data from these stations provided us an opportunity to study the attenuation characteristics for the first time in the region.

2 SEISMOTECTONICS OF SIKKIM HIMALAYA

The Himalayan orogenic belt is one of the most seismically active continent–continent collision zones in the world, where the Indian Plate continues to underthrust the Eurasian Plate since the hard collision ∼50 Ma ago. The 2500-km-long stretch along the strike of the Himalaya can be divided into different tectonically active segments that exhibit structural variations from west to east (Kayal 2001). Within the eastern Himalaya, the province of Sikkim is bounded by Bhutan in the east, Nepal in the west and Tibet in the north. Having experienced moderate seismicity in the past, this region has been designated as zone IV in the seismic zonation map of India (IS 2002). The great Bihar–Nepal earthquake (*M* 8.4) of 1934 had its epicentre to the west of Sikkim and caused an intensity of VIII on the Modified Mercalli scale. Also, in the year 1988, another earthquake having a magnitude of 6.6 occurred in the vicinity of the 1934 earthquake and generated an intensity of VII within the Sikkim–Himalaya (Kayal 2001) region. More recently, on 2011 September 18, an earthquake of M_w 6.9 occurred in the northwestern part of Sikkim, at the Nepal–India border. This is the largest earthquake ever in the vicinity of Sikkim. The prominent tectonic features in the Sikkim region are the Main Boundary Thrust (MBT) and a peculiarly overturned Main Central Thrust (MCT), in addition to the NW–SE-trending subparallel Gangtok and Tista lineaments and the WNW–ENE-trending Goalpara lineament (GSI 2000; fig. 1). It is observed that earthquakes in this region are generally confined between the MBT and the MCT, without being associated with either (Kayal 2001; De & Kayal 2004; Hazarika *et al.* 2010). While the entire Himalayan front is generally characterized by shallow angle thrust faulting, earthquake focal mechanisms in this region are predominantly of strike-slip type, in conformity with a right-lateral strike-slip mechanism along the NW-trending Tista and Gangtok lineaments (Hazarika *et al.* 2010).

3 DATA

The National Geophysical Research Institute, Hyderabad, has operated 11 broad-band seismic stations in the Sikkim region from 2004 October to 2010 February, along a near north–south profile from Mangpoo in West Bengal to Thangu in northern Sikkim. Each station hosts either an STS2 or KS2000 broad-band seismometer connected to Reftek data acquisition systems. Data are recorded in continuous mode at 20 samples per second. In this study, high-quality waveforms from 68 local earthquakes shallower than 45 km, that occurred during the period 2006–2007 are selected for analysing the attenuation structure. These earthquakes in the magnitude range of 2–4.5 are well located using the SEISAN software (Havskov & Ottemueller 2003) and relocated using the hypoDD (Waldhauser 2001) relocation program (Hazarika *et al.* 2010). To ensure location accuracies, waveforms of events recorded by a minimum of three stations are used. As a consequence, 592 seismograms from eight stations qualified for the analysis. Table 1 lists the hypocentral parameters of the earthquakes used, along with their errors and Fig. 1 shows the epicentral distribution of the events and the stations used in this study. Both the vertical and north-south components of all the selected events are considered after detrending the seismograms and filtering them using five different central frequencies of 1.5 (1–2 Hz), 3 (2–4 Hz), 5 (4–6 Hz), 7 (6–8 Hz) and 9 (8–10 Hz) utilizing a butterworth bandpass filter. Fig. 2 shows an example of the original and filtered seismograms of an event that occurred on 2006 May 3.

4 METHODOLOGY

In this study, the coda wave attenuation (Q_c) has been estimated using the single backscattering model of Aki & Chouet (1975). According to this model, the coda waves are interpreted as backscattered body waves generated by numerous heterogeneities present in the Earth's crust and upper mantle. It implies that scattering is a weak process and that outgoing waves are scattered only once before reaching the receiver. Under this assumption, for a central frequency '*f*' over a narrow bandwidth signal, the coda amplitudes $A_c(f, t)$, in a seismogram can be expressed as a function of the lapse time '*t*' measured from the origin time of the seismic event as (Aki 1980)

$$A_c(f, t) = S(f)t^{-a}\exp(-\pi f t/Q_c), \quad (1)$$

where $S(f)$ is the source function at frequency *f*. This function is considered as constant, since it is independent of time and radiation pattern and hence unaffected by factors influencing energy loss in the medium. Term '*a*' is the geometrical spreading factor which equals unity for body waves and Q_c is the apparent quality factor of coda waves representing the attenuation in a medium. By taking the natural logarithm on both sides of eq. (1) we get

$$\ln[A_c(f, t)t] = \ln S(f) - (\pi f/Q_c)t. \quad (2)$$

Table 1. Hypocentral parameters of earthquakes used in this study. ERX: error in longitude; *M*l: magnitude; rms: root mean squared error; ERY: error in latitude; ERZ: error in depth.

Date	Origin time	Latitude	Longitude	Depth (km)	*M*l	rms (s)	ERX (m)	ERY (m)	ERZ (m)
20/01/2006	21:41:10.36	27.717	88.245	33.9	2.8	0.08	45.2	30.1	51.6
02/02/2006	00:17:45.04	27.264	88.632	44.5	2.9	0.02	64.0	45.2	44.9
13/02/2006	02:37:43.92	27.551	88.449	21.1	2.4	0.10	211.2	276.0	174.9
14/02/2006	03:01:11.55	27.402	88.438	6.1	2.0	0.07	43.1	35.5	87.5
16/02/2006	17:56:21.44	27.838	88.08	26.2	2.5	0.07	42.2	73.5	77.2
20/02/2006	20:32:04.26	27.415	88.503	13.3	2.2	0.09	45.2	30.1	51.6
26/02/2006	22:15:21.82	27.525	88.256	11.3	2.4	0.10	64.0	45.2	44.9
14/03/2006	19:34:10.43	27.289	88.457	12.9	2.3	0.04	43.6	33.6	25.1
05/04/2006	07:54:49.19	27.33	88.619	19.4	2.1	0.02	43.9	14.1	47.3
05/04/2006	15:11:45.39	27.683	88.551	5.4	2.5	0.14	148.7	218.7	148.8
17/04/2006	22:57:54.22	27.308	88.6	25.4	2.6	0.07	50.6	112.1	59.8
24/04/2006	06:42:35.88	27.908	87.743	40.1	2.9	0.09	171.0	170.9	123.0
25/04/2006	14:45:17.11	27.521	88.531	18.2	2.5	0.19	728.7	418.3	638.9
27/04/2006	21:24:36.32	27.331	88.604	6.7	3.0	0.14	290.2	338.1	326.6
03/05/2006	22:58:33.97	27.364	88.851	15.3	3.4	0.11	460.8	223.7	365.1
08/05/2006	13:46:12.26	27.702	88.897	15	3.0	0.07	237.6	179.4	131.6
12/05.2006	03:25:45.44	27.252	88.673	16.6	3.1	0.04	178.2	195.6	104.9
14/05/2006	21:45:54.29	27.054	88.7	26	2.6	0.09	171.0	170.9	123.0
15/05/2006	02:15:55.07	27.242	88.7	26	2.6	0.09	238.4	210.9	140.7
25/05/2006	03:13:57.09	27.374	88.532	18.9	2.8	0.11	228.6	373.0	267.8
02/06/2006	17:17:05.03	27.364	88.517	13.1	2.7	0.08	438.3	527.3	234.3
14/06/2006	10:32:18.79	27.017	88.007	31.1	2.4	0.03	507.5	538.4	942.0
23/06/2006	04:47:43.04	27.55	88.661	32.6	2.8	0.08	237.6	179.4	131.6
23/06/2006	22:07:52.07	27.42	88.771	18.8	3.6	0.09	3162.0	1187.2	1469.1
04/07/2006	15:18:29.07	27.262	88.852	10.3	2.5	0.11	117.9	169.6	119.8
18/07/2006	13:22:29.00	27.217	88.748	36.5	2.8	0.13	150.7	252.5	183.7
27/07/2006	17:41:22.81	27.622	88.924	10.5	2.5	0.06	189.3	191.3	117.6
07/08/2006	22:19:01.03	27.301	88.816	17.0	3.0	0.05	652.4	476.7	466.0
19/08/2006	16:49:44.09	27.27	88.012	40.4	2.5	0.07	385.8	286.1	328.0
08/09/2006	02:58:38.05	27.769	88.005	27.6	2.6	0.1	1277.2	1162.1	1303.0
01/10/2006	12:08:32.09	27.372	88.509	22.4	2.9	0.07	1162.2	557.2	865.4
08/10/2006	05:07:25.06	27.373	88.837	26.4	2.5	0.13	246.6	378.1	216.0
25/10/2006	09:53:34.89	27.54	88.499	32.5	3.3	0.11	45.1	23.8	38.3
08/11/2006	09:45:10.00	27.502	88.733	40.2	3.5	0.13	290.2	338.1	326.6
18/11/2006	16:20:37.47	27.801	87.944	22.1	2.8	0.1	728.7	418.3	638.9
24/11/2006	07:15:01.32	27.143	88.282	39.1	2.5	0.04	250.8	43.1	47.0
26/11/2006	23:46:27.05	27.498	88.253	26.8	2.0	0.11	728.7	418.3	638.9
07/12/2006	14:46:50.05	27.252	88.778	24.2	3.1	0.1	1013.1	1477.2	524.0
23/12/2006	13:27:24.00	27.465	88.643	34.6	3.4	0.08	263.5	681.5	299.4
31/12/2006	08:10:25.00	27.399	88.485	17.9	2.6	0.12	1561.0	713.9	582.7
02/01/2007	16:13:41.00	27.782	87.894	21.1	2.6	0.11	52.7	34.7	31.2
08/01/2007	18:52:43.01	27.793	87.791	25.6	2.5	0.02	55.0	51.9	64.9
11/01/2007	22:58:23.04	27.461	88.935	23.5	3.4	0.08	1162.2	557.2	865.4
06/02/2007	21:39:01.01	27.867	87.931	9.1	4.0	0.04	44.2	17.3	18.2
11/02/2007	16:22:41.09	27.427	88.733	34.3	2.4	0.1	150.7	252.5	183.7
14/02/2007	15:33:41.02	27.413	88.725	36.1	2.7	0.14	191.7	259.6	163.4
05/04/2007	18:20:44.08	27.173	89.077	15.5	2.5	0.09	728.7	418.3	638.9
06/05/2007	23:54:01.03	27.472	88.669	28.4	3.7	0.09	1801.2	912.2	1049.8
07/05/2007	17:04:47.08	27.308	88.048	31.7	2.7	0.08	237.6	179.4	131.6
16/05/2007	07:17:27.94	27.053	88.902	28.6	3.5	0.1	630.9	479.0	654.0
18/05/2007	11:42:49.43	27.292	88.43	19.6	3.2	0.12	2735.6	1438.0	1736.4
19/05/2007	12:41:48.52	27.316	88.482	18.5	2.4	0.04	117.9	169.6	119.8
20/05/2007	15:29:45.51	27.289	88.545	18.2	3.0	0.13	798.0	652.4	293.3
21/05/2007	19:59:56.87	27.307	88.527	21	2.2	0.09	652.4	476.7	466.0
22/05/2007	05:24:43.82	27.309	88.513	16.4	2.2	0.1	662.1	1196.2	1966.3
23/05/2007	12:54:42.07	27.304	88.519	17.2	2.4	0.03	451.8	515.6	681.5
23/05/2007	13:31:40.54	27.328	88.636	5.6	2.2	0.02	58.0	37.5	44.2
24/05/2007	16:27:16.66	27.311	88.55	19.5	3.2	0.12	678.9	484.4	474.2
16/06/2007	12:04:31.19	27.347	88.813	23.7	2.7	0.11	86.5	117.4	108.2
25/06/2007	13:11:28.98	27.132	88.352	39.3	3.2	0.03	229.7	43.4	46.6
04/07/2007	22:10:10.52	27.306	88.541	13.4	2.9	0.03	52.7	23.8	27.9
03/08/2007	03:50:42.39	27.324	88.782	28.6	3.9	0.08	50.6	112.1	59.8
11/08/2007	14:35:53.03	27.421	87.936	34.4	4.3	0.13	171.0	170.9	123.0
16/08/2007	09:41:02.95	27.665	88.609	32.4	2.4	0.08	425.5	424.1	524.3
27/08/2007	11:57:40.82	27.461	88.624	30	2.9	0.07	385.8	286.1	328.0
28/08/2007	03:03:41.67	27.076	89.07	40.8	3.7	0.08	460.8	223.7	365.1
05/09/2007	05:07:13.31	27.359	88.785	34.7	2.8	0.1	1162.2	557.2	865.4
17/09/2007	20:35:14.92	27.334	88.472	18.4	2.2	0.09	371.7	782.0	779.8

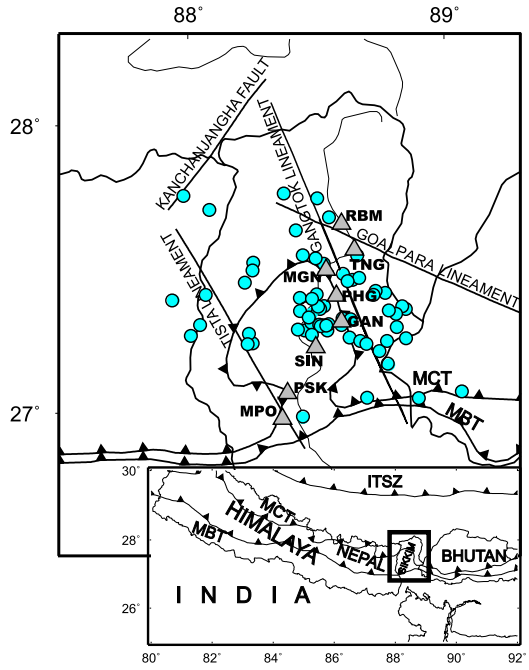

Figure 1. Map of Sikkim Himalaya with the major tectonic features showing the locations of earthquakes (circles) and seismic stations (triangles) used in this study. Bottom panel shows a simplified tectonic map of central and eastern Himalaya enclosing Sikkim with an open rectangle.

This being a linear equation with slope $-\pi f/Q_c$ enables estimation of Q_c in a simple manner.

The *P*-wave (Q_α) and the *S*-wave attenuation (Q_β) factors are estimated based on the concept that coda waves consist of scattered *S* waves from random heterogeneities in the Earth (Aki 1969; Aki & Chouet 1975; Sato 1977). The coda normalization method (Aki 1980) is based on the empirical observation that the coda spectral amplitude at lapse times greater than twice the *S*-wave travel-time is proportional to the source spectral amplitude of *S* waves at distances less than 100 km (Yoshimoto *et al.* 1993; Kim *et al.* 2004). Therefore, the source effects, the common instrument and site responses are removed by normalizing the *S*-wave spectra to those of the coda. The spectral amplitude, $A_c(f, t_c)$, of the coda at a lapse time t_c can be written as (Aki 1980)

$$A_c(f, t_c) = S_s(f)P(f, t_c)G(f)I(f), \tag{3}$$

where f is the frequency, $S_s(f)$ is the source spectral amplitude of *S* waves, $P(f, t_c)$ is the coda excitation factor, $G(f)$ is the site amplification factor and $I(f)$ is the instrumental response. The spectral amplitude of the direct *S* wave, $A_s(f, r)$, can be expressed as

$$A_s(f, r) = R_{\theta\phi}S_s(f)r^{-\gamma}\exp[-\pi f r/Q_\beta(f)V_s]G(f, \psi)I(f), \tag{4}$$

where $R_{\theta\phi}$ is the source radiation pattern and γ denotes the geometrical spreading exponent. $Q_\beta(f)$ is the quality factor of *S* waves, V_s is the average *S*-wave velocity and ψ is the incidence angle of *S* waves. On dividing eq. (4) by eq. (3), taking the logarithm and simplifying, we get the average for a hypocentral distance range $r \pm \Delta r$ as (Yoshimoto *et al.* 1993)

$$\ln\left[\frac{A_s(f, r)r^\gamma}{A_c(f, t_c)}\right]_{r\pm\Delta r} = -\left[\frac{\pi f}{Q_\beta(f)V_s}\right]r + \text{const}(f). \tag{5}$$

Eq. (5) is obtained under the assumptions that the contribution of $R_{\theta\phi}$ disappears by averaging over many different focal plane solutions and the ratio $G(f, \psi)/G(f)$ becomes independent of ψ by averaging over many earthquakes (Yoshimoto *et al.* 1993). The quality factor for *S* waves can be obtained from the linear regression of $\ln[A_s(f, r)r^\gamma]/[A_c(f, t_c)]_{r\pm\Delta r}$ versus r by means of a least-squares method. Using a similar equation, the quality factor for the *P* waves can be obtained as (Yoshimoto *et al.* 1993)

$$\ln\left[\frac{A_p(f, r)r^\gamma}{A_c(f, t_c)}\right]_{r\pm\Delta r} = -\left[\frac{\pi f}{Q_\alpha(f)V_p}\right]r + \text{const}(f). \tag{6}$$

The quality factor for *P* waves can be obtained from the linear regression of $\ln[A_p(f, r)r^\alpha]/[A_c(f, t_c)]_{r\pm\Delta r}$ versus r by means of a least-squares method, similar to that for *S* waves.

To estimate Q_i and Q_s, we use the formula of Wennerberg (1993) and the model of Zeng *et al.* (1991). According to Zeng *et al.* (1991), the observed value of Q_c can be written in terms of Q_i and Q_s as follows:

$$\frac{1}{Q_c} = \frac{1}{Q_i} + \frac{1 - 2\delta(\tau)}{Q_s}, \tag{7}$$

where $\delta(\tau)$ is $-1/(4.44 + 0.738), \tau = \omega t/Q_s$, ω is the angular frequency and t is the lapse time. Assuming Q_β as the quality factor of the direct wave evaluated in the Earth volume equivalent to the volume sampled by the coda waves, the equation can be written as (Wennerberg 1993)

$$\frac{1}{Q_s} = \frac{1}{2\delta(\tau)}\left[\frac{1}{Q_\beta} - \frac{1}{Q_c(\tau)}\right], \tag{8}$$

$$\frac{1}{Q_i} = \frac{1}{2\delta(\tau)}\left[\frac{1}{Q_c}(\tau) + \frac{2\delta(\tau) - 1}{Q_\beta}\right]. \tag{9}$$

If Q_c is measured as a function of lapse time t, Q_i and Q_s can be estimated using eqs (7)–(9), where Q_β is measured as a function of distance.

5 RESULTS AND DISCUSSION

5.1 Coda wave attenuation Q_c

The coda quality factor Q_c was estimated using both the vertical and horizontal components of the seismograms using the rms amplitude of the coda waves in a window length of 50 samples for different lapse time windows of 20, 30, 40, 50 and 60 s duration. To avoid interference with *S* waves, the beginning of the coda window (lapse time) is taken after twice the *S*-wave traveltime (Rautian & Khalturin 1978). It has been demonstrated by various workers (e.g. Havskov & Ottemoller 2003; Mukhopadhyay & Sharma 2010; Gupta *et al.* 2012) that the coda window length should be large enough to obtain stable results. Fig. 3 shows the variation of $\ln[A_c(f,t)t]$ with lapse time t, together with the least-square fit lines, for the example seismogram shown in Fig. 2. For each central frequency, the range of slopes and intercepts which are consistent with the data at the 95 per cent confidence level are also indicated. Using the slope of the least-square fit line, we calculated the values of Q_c as described in the methodology section and plotted them with respect to the central frequency (Fig. 4).

To decipher the dependence of Q_c on lapse time, different values of Q_c obtained for several lapse time windows are plotted in Fig. 5 for both the vertical as well as the horizontal components. Table 2 summarizes the Q_c values at different central frequencies calculated using different lapse time windows for both the vertical and horizontal components. Fig. 5 reveals that the values of Q_c tend to increase with frequency as well as lapse time. Previous studies attribute the increase of Q_c with lapse time to increase of Q_c with

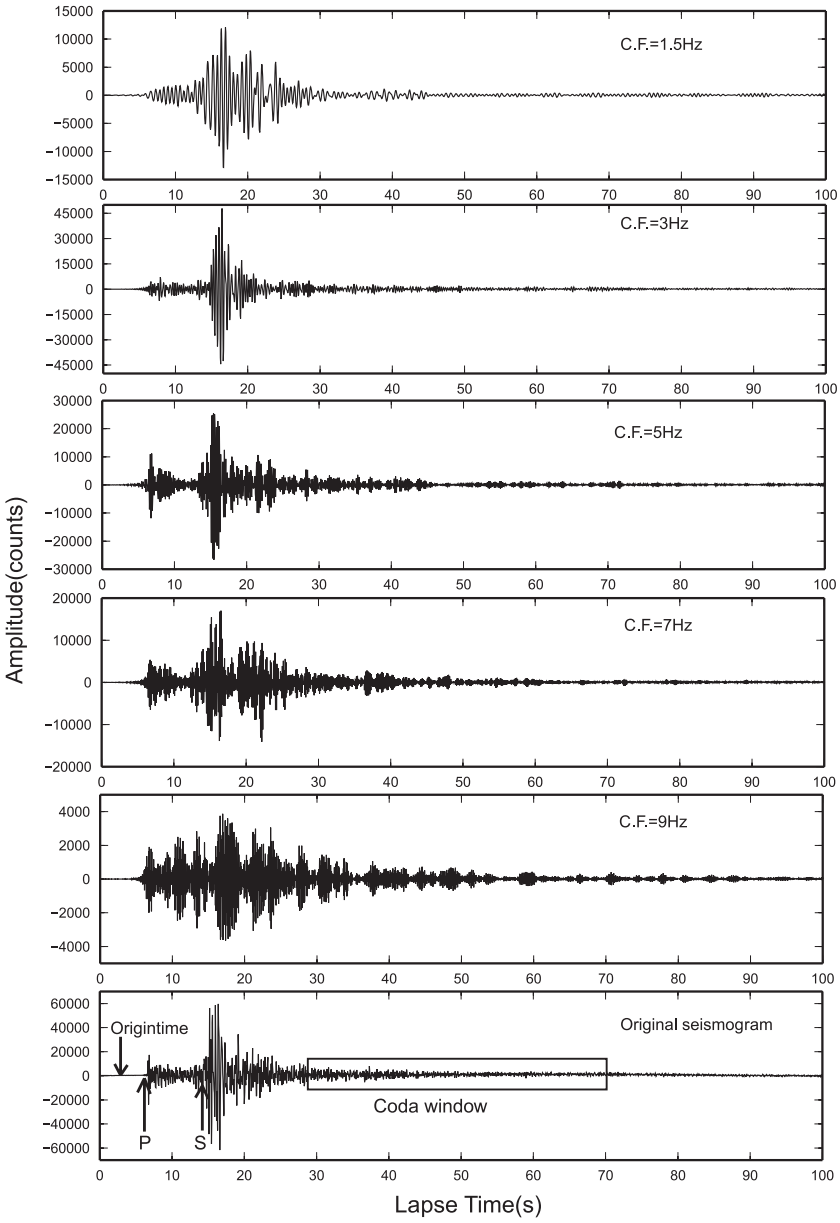

Figure 2. Examples of original and filtered seismograms recorded at seismic station MPO due to an earthquake that occurred on 2006 May 3.

depth (Ibanez *et al.* 1990; Del Pezzo & Patane 1992; Akinci *et al.* 1994; Gupta *et al.* 1998; Giampiccolo *et al.* 2002). As discussed in the next section, our estimates of Q_c for three different depth ranges validates this for the Sikkim Himalaya. Also, the value of Q_c increases with lapse time and the Q_c values obtained from the horizontal and vertical components coincide at the lapse time window of 40 s (Fig. 5). It seems from this result that the values of Q_c are independent of the seismogram component. Hence, we consider the Q_c values obtained for the 40 s lapse time window as the standard value for further comparison of the results. The estimated Q_c values show a strong frequency dependence, with the Q_c values obtained for five central frequencies showing an increase with frequency (Fig. 4). Table 3 shows the different values of Q_c estimated at various stations for different central frequencies. The variations in the values of Q_c at various stations range from 187 to 1623 at PSK, 156 to 1464 at PHG, 142 to 1482 at SIN, 208 to 2112 at TNG, 246 to 1620 at MPO, 180 to 1650 at MGN, 250 to 1749 at RBM and 203 to 1727 at GAN, for frequencies corresponding to 1.5 Hz and 9 Hz, respectively. The lateral variation of the estimated Q values may be attributed to heterogeneities present in the region and/or difference in the distances of the events from the recording stations. The average value of Q_c varies from 197 (at 1.5 Hz) to 1678 (at 9 Hz). Further, these variations of Q_c with frequency are represented using the power-law $Q_c = Q_0 f^n$ (Fig. 4). For Sikkim Himalaya, this relation between the average Q_c value and frequency is $Q_c = (189 \pm 1.5) f^{(1.2 \pm 0.01)}$. The obtained value of 'n' being greater than unity indicates a strong dependence of Q_c with frequency. The Q_c values obtained for Sikkim seem comparable with results from other tectonic regions (Fig. 6). Fig. 6 also reveals that at high frequencies, the Q_c values for Sikkim are a little higher compared to other regions. When compared with other segments of Himalaya, like the Northwest Himalaya, Garhwal Himalaya and Kumaun Himalaya, the value of Q_c in Sikkim falls within the same range; with the Chamoli region showing slightly lower values (Fig. 6). A slightly

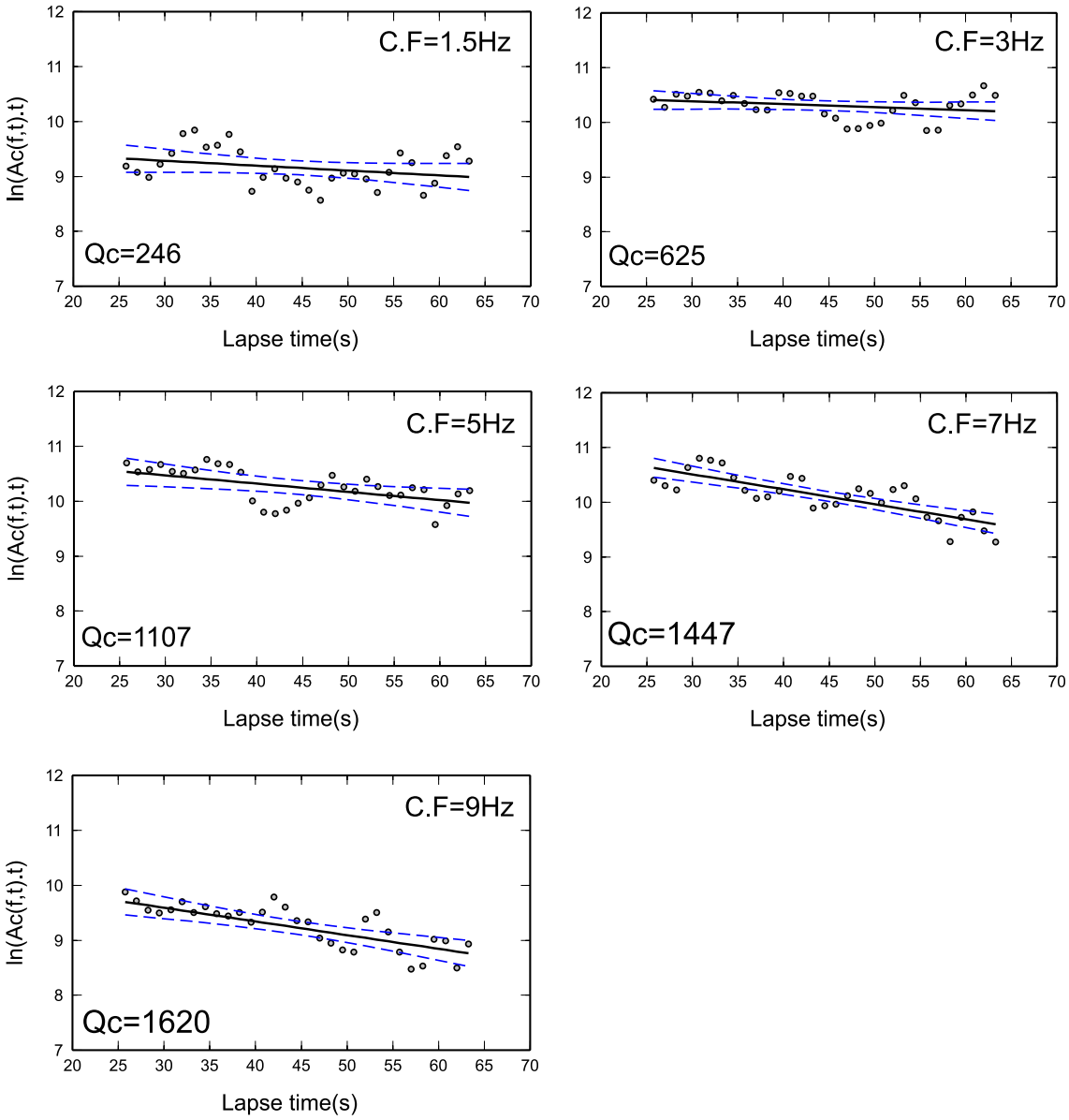

Figure 3. Variation of $\ln(A_c(f,t).t)$ with lapse time t at five different central frequencies for the seismogram shown in Fig. 2, for a 40 s coda window. Solid line is the least-square fit at 95 per cent confidence interval. Dashed lines show the upper and lower bounds of the fit.

higher Q_c in Sikkim may be attributed to the fact that the seismic activity in this region is comparatively lower than the other sections of Himalaya.

5.2 Variation of Q_c with focal depth

We also estimated the depth dependence of the coda quality factor by classifying the data into three groups based on the focal depth (D) of the earthquakes: (1) 12 events with $D < 15$ km; (2) 35 events with $15 \leq D < 30$ km and (3) 21 events with $30 \leq D < 45$ km. It is observed that the estimated Q_c values change with depth (Table 4), with events having shallow depth showing lower values compared to those from deeper depths. This observation of a larger attenuation in the upper crust can be related to higher seismic activity in the upper crust compared to the lower crust. As seen globally, the Q values are low in seismically active tectonic regions. The factor n (>1 in this study) that denotes frequency dependence is also high for shallow depths compared to larger depths implying that the upper crust is more heterogeneous compared to the lower. Although most of the Q_c values seem to increase with depth, we found lower Q_c values at higher frequencies (7 Hz and 9 Hz) at deeper depths compared to those at shallow depths. This suggests that the degree of frequency dependence is less at deeper depths compared to the shallower ones. This fact indicates that the lower crust is less heterogeneous than the upper crust. It was earlier proposed that the lapse time dependency of Q_c can be interpreted in terms of variation of attenuation with earthquake focal depth (Roecker *et al.* 1982; Kvamme & Havskov 1989; Ibanez *et al.* 1990; Akinci 1994; Gupta *et al.* 1998; Mukhopadhyay & Sharma 2010). Results from this study also indicate an increase in Q_c with lapse time as well as depth. The lapse time dependency of Q_c may occur due to an inappropriate assumption of the back scattering model (Padhy *et al.* 2009; Mukhopadhyay & Sharma 2010). Woodgold (1994) proposed

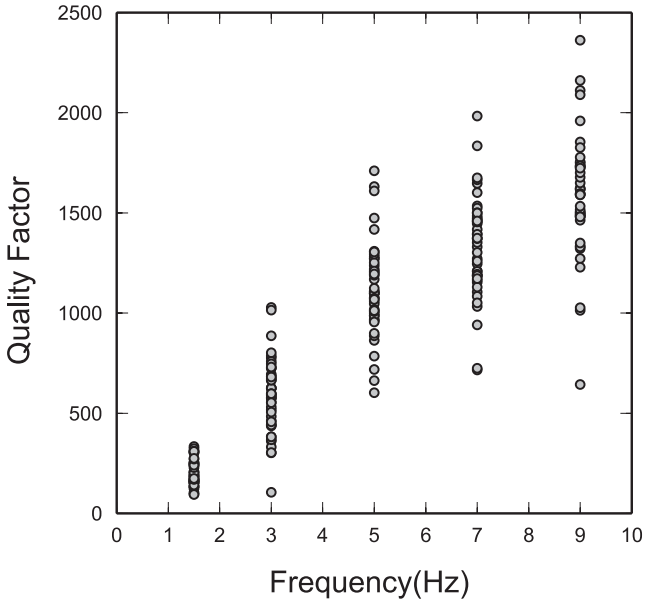

Figure 4. Variation of Q_c with respect to frequency.

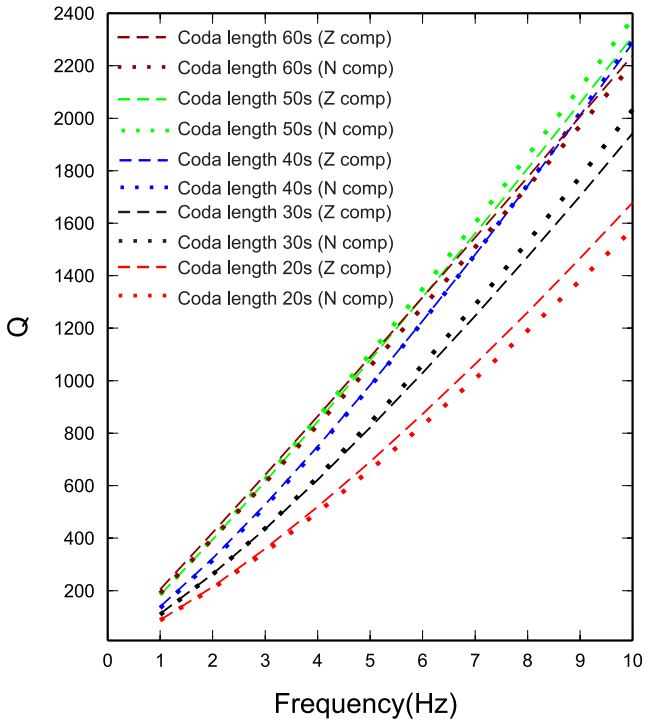

Figure 5. Q_c variation for different coda lengths for both vertical (dashed) and NS (dotted) components of seismograms.

that lapse time dependency of Q_c could be due any of the following reasons; non-zero source-receiver distance; non-isotropic scattering; scattering from below the crust; multiple scattering; or increase of Q_c with depth or with distance from both the source and receiver. Since lapse time-dependent attenuation can be explained by depth dependency of attenuation, we conclude that our assumptions about the backscattering model is valid for the Sikkim Himalaya.

5.3 Body wave attenuation Q_α and Q_β

Adopting the coda normalization method (Yoshimoto *et al.* 1993) we estimated the attenuation quality factor for P (Q_α) and S waves (Q_β). This was done by first estimating Q_α and Q_β values individually for each station and then determining the average values by combining measurements from all the stations. For tectonically stable regions where earthquake data are limited, many workers have estimated the Q_α and Q_β values by combining the waveforms of multiple events recorded at multiple stations. However, in view of sufficient amount of data, we calculate Q_α and Q_β values for individual stations. For this purpose, the rms amplitudes for P and S waves are picked from the filtered seismograms and normalized by the coda wave amplitude. The spectral amplitudes for direct P and S wave arrivals are determined from the vertical and N–S components of the filtered seismograms, respectively. Geometric spreading is assumed to be inversely proportional to the hypocentral distance, since the selected events are within a radius of 100 km from the seismic stations. We measured the coda spectral amplitudes using the rms amplitude within a time window of 5 s centred at $t_c = 40$ s, using the same component of arrivals analysed for coda normalization for each frequency band. As our event station distance is within 100 km, choice of a 40 s t_c beyond twice the direct S-wave traveltime is sufficient to calculate the coda wave amplitude with a good signal-to-noise ratio. We then plot the $\ln[(A_{p,s}/A_c)r]$ (p for Q_α and s for Q_β) with respect to the hypocentral distance r (in kilometres) at five different central frequencies (1.5 Hz, 3 Hz, 5 Hz, 7 Hz and 9 Hz) for all the stations and use a least-squares approach for obtaining the best fit results. The range of slopes and intercepts of the least-square fit is calculated at the 95 per cent confidence level. Using the slope of the least-square line, the values of Q_α and Q_β are estimated from eqs (5) and (6). Examples of the least-square regression along with the error bounds for different central frequencies are shown inFigs 7 and 8 for station MPO, corresponding to Q_α and Q_β, respectively. An average P-wave velocity of 6.66 km s^{-1} and S-wave velocity of 3.6 km s^{-1} (Hazarika *et al.* 2010) have been used to evaluate Q_α and Q_β, respectively.

For individual stations, the estimated values of Q_α and Q_β at different central frequencies are summarized in Tables 5 and 6, respectively, along with their 1σ errors. Although most of these results reveal good estimates, some values have large errors. Since we consider only the average values for further comparison of results, a few bad values do not largely effect our interpretation. Increase of Q values with frequency at almost all the stations supports the frequency-dependent nature of Q. To assess the regional variation of the Q values and their dependence on frequency, we obtain power-law relations for individual seismic stations. We note that the estimated values of Q show a variation, probably due to the presence of heterogeneities. At stations PSK, MPO and SIN, located in the southern part of the Sikkim Himalaya, the Q values are found to be higher compared to the stations located in the central part like PHG, RBM and TNG, suggesting that the middle part of Sikkim Himalaya, mainly to the north of MBT, is tectonically more active. The average value of Q_α is 141 at a central frequency of 1.5 Hz and 639 at a central frequency of 9 Hz. Similarly, the average value of Q_β is 143 at a central frequency of 1.5 Hz and 1108 at a central frequency of 9 Hz. This frequency-dependent attenuation in Sikkim is comparable to that observed in other tectonic regions such as Kanto (Japan; Yoshimoto *et al.* 1993), Egypt (Abdel-Fattah 2009), Bhuj (India; Padhy 2009), Koyna (India; Sharma *et al.* 2007), Kachchh (India; Sharma *et al.* 2008), northeast India (Padhy & Subhadra 2010) and Kumaun Himalaya (Singh *et al.* 2012). To quantify the

Table 2. Estimated values of coda quality factors for vertical and North–South components for different lapse times at five selected central frequencies.

C.F. (Hz)	Component	Coda length (s)				
		20	30	40	50	60
1.5	Z	134 ± 23	161 ± 28	197 ± 36	242 ± 50	274 ± 47
	N	139 ± 31	159 ± 21	195 ± 15	222 ± 30	266 ± 46
3	Z	368 ± 119	505 ± 115	598 ± 83	758 ± 160	730 ± 116
	N	358 ± 78	486 ± 76	589 ± 95	628 ± 42	676 ± 42
5	Z	899 ± 158	955 ± 148	1204 ± 207	1252 ± 131	1305 ± 196
	N	710 ± 151	1030 ± 258	1134 ± 154	1181 ± 206	1183 ± 93
7	Z	1051 ± 148	1187 ± 208	1475 ± 103	1500 ± 161	1460 ± 240
	N	1003 ± 212	1280 ± 205	1487 ± 199	1498 ± 160	1480 ± 157
9	Z	1229 ± 310	1516 ± 153	1678 ± 215	1778 ± 241	1776 ± 237
	N	1304 ± 242	1497 ± 188	1735 ± 230	1744 ± 165	1785 ± 90

Table 3. Values of coda quality factor for different central frequencies calculated using vertical components at different seismic stations for a 40 s lapse time window.

Station code	1.5	3	5	7	9	$Q_c = Q_0 f^n$
PSK	187 ± 53	555 ± 190	1237 ± 298	1485 ± 382	1623 ± 452	$(129 \pm 3.1) f^{(1.2 \pm 0.02)}$
GAN	203 ± 115	576 ± 177	1077 ± 211	1601 ± 777	1727 ± 577	$(136 \pm 1.4) f^{(1.2 \pm 0.01)}$
MGN	180 ± 54	776 ± 253	1098 ± 304	1524 ± 508	1650 ± 451	$(142 \pm 6.5) f^{(1.2 \pm 0.04)}$
MPO	246 ± 75	625 ± 182	1107 ± 265	1447 ± 399	1620 ± 451	$(176 \pm 1.6) f^{(1.1 \pm 0.01)}$
PHG	156 ± 40	625 ± 193	1012 ± 240	1395 ± 291	1464 ± 538	$(118 \pm 4.5) f^{(1.3 \pm 0.03)}$
RBM	250 ± 65	589 ± 200	1710 ± 799	1330 ± 678	1749 ± 924	$(178 \pm 9.3) f^{(1.1 \pm 0.04)}$
SIN	142 ± 58	457 ± 130	1109 ± 335	1374 ± 414	1482 ± 393	$(94 \pm 2.7) f^{(1.4 \pm 0.02)}$
TNG	208 ± 73	579 ± 173	1282 ± 378	1647 ± 710	2112 ± 858	$(132 \pm 1.1) f^{(1.3 \pm 0.01)}$

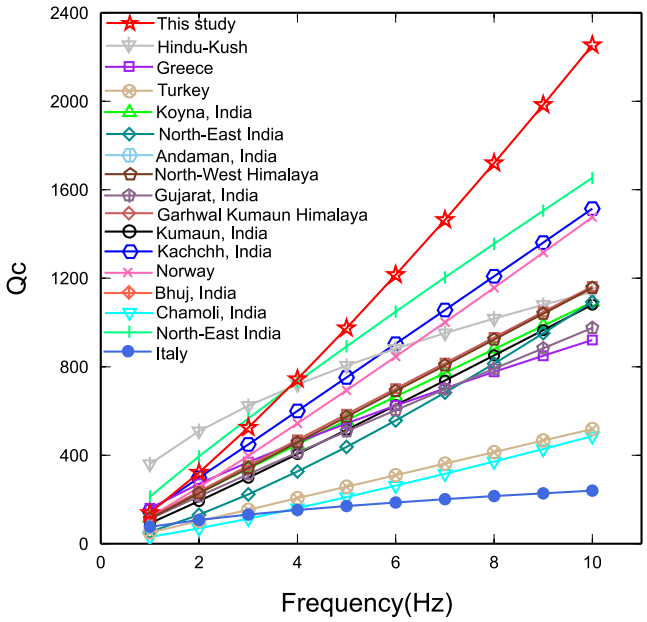

Figure 6. Comparison of estimated Q_c (at 40 s coda length) variation with those from other tectonic regions. Sources of the reported values : Hindu-Kush (Roecker *et al.* 1982); Greece (Bauskoutas *et al.* 1998); Turkey (Akinci *et al.* 1996), Koyna, India (Sharma *et al.* 2007); North-East India (Padhy & Subhadra 2010); Andaman, India (Padhy *et al.* 2011); Gujarat, India (Gupta *et al.* 2012); Garhwal–Kumaun Himalaya (Mukhopadhyay & Sharma 2010); Kumaun, India (Paul *et al.* 2003); Kachchh, India (Sharma *et al.* 2008); Norway (Kvamme & Havskov); Bhuj, India (Padhy 2009); Chamoli, India (Mandal *et al.* 2001); North-East India (Padhy & Subhadra 2010); Italy (Tuve *et al.* 2006).

relation between frequency and Q, the average values of Q_α and Q_β are fit using the same power law used for Q_c in the previous section. The relations are found to be

$$Q_\alpha = (96 \pm 0.9) f^{(0.94 \pm 0.01)} \text{ and } Q_\beta = (100 \pm 1.4) f^{(1.16 \pm 0.01)}.$$

Figs 9 and 10 show the frequency dependence of Q_α and Q_β for the Sikkim Himalaya, along with such relations for other tectonic regions globally. Slightly higher Q_α and Q_β values for Sikkim compared to other tectonically active regions reiterates the lower seismic activity in the region. It can be seen from the figures that for the Saurashtra region in India, the Q_α and Q_β values are high, commensurate with the low level of seismicity (Chopra *et al.* 2010). For the South Central Korea region, the Q value reported (Kim *et al.* 2004) is less frequency dependent, as this region is seismically stable. In this region also, the Q values are higher compared to those in seismically active regions. Our observation of Q_β/Q_α being >1 for the whole frequency range means that the attenuation of P waves is stronger than that of S waves in this region. A plot of our values of S-wave attenuation versus P-wave attenuation at 1 Hz, together with the values obtained for different regions by other workers, suggests that $Q_\beta > Q_\alpha$ is an observation valid for most tectonic regions (Fig. 11). Only few examples exist where Q_β/Q_α is less than or equal to unity. The ratio Q_β/Q_α varies widely from 0.6 to 1.85 and is larger than unity at frequencies higher than 1 Hz (Sato 1984). Yashimoto *et al.* (1998) reported that the ratio Q_β/Q_α has values between 1.3 to 2.9 in Western Nagano Japan. From Fig. 11 also, it is distinct that the values of Q_β/Q_α are maximum for Western Nagano, Japan. Yashimoto *et al.* (1998), reported that Q_α values in Western Nagano are three to four times smaller than those reported from past studies in Japan, probably due to the depth variation of Q_α and/or possible increase in attenuation due to the occurrence of the

Table 4. Depth variation of Q_c at different central frequencies along with the respective power laws defining frequency dependency.

C.F. (Hz)	Depth < 15 km	15 km ≤ Depth < 30 km	30 km ≤ Depth < 45 km
1.5	175 ± 53	217 ± 88	266 ± 106
3	540 ± 177	688 ± 277	833 ± 387
5	1153 ± 340	1404 ± 698	1419 ± 491
7	1401 ± 438	1685 ± 560	1597 ± 553
9	1677 ± 726	1963 ± 985	1736 ± 720
$Q_c = Q_0 f^n$	$(119 \pm 2.1) f^{(1.3 \pm 0.01)}$	$(153 \pm 3.3) f^{(1.2 \pm 0.02)}$	$(212 \pm 6.6) f^{(1 \pm 0.01)}$

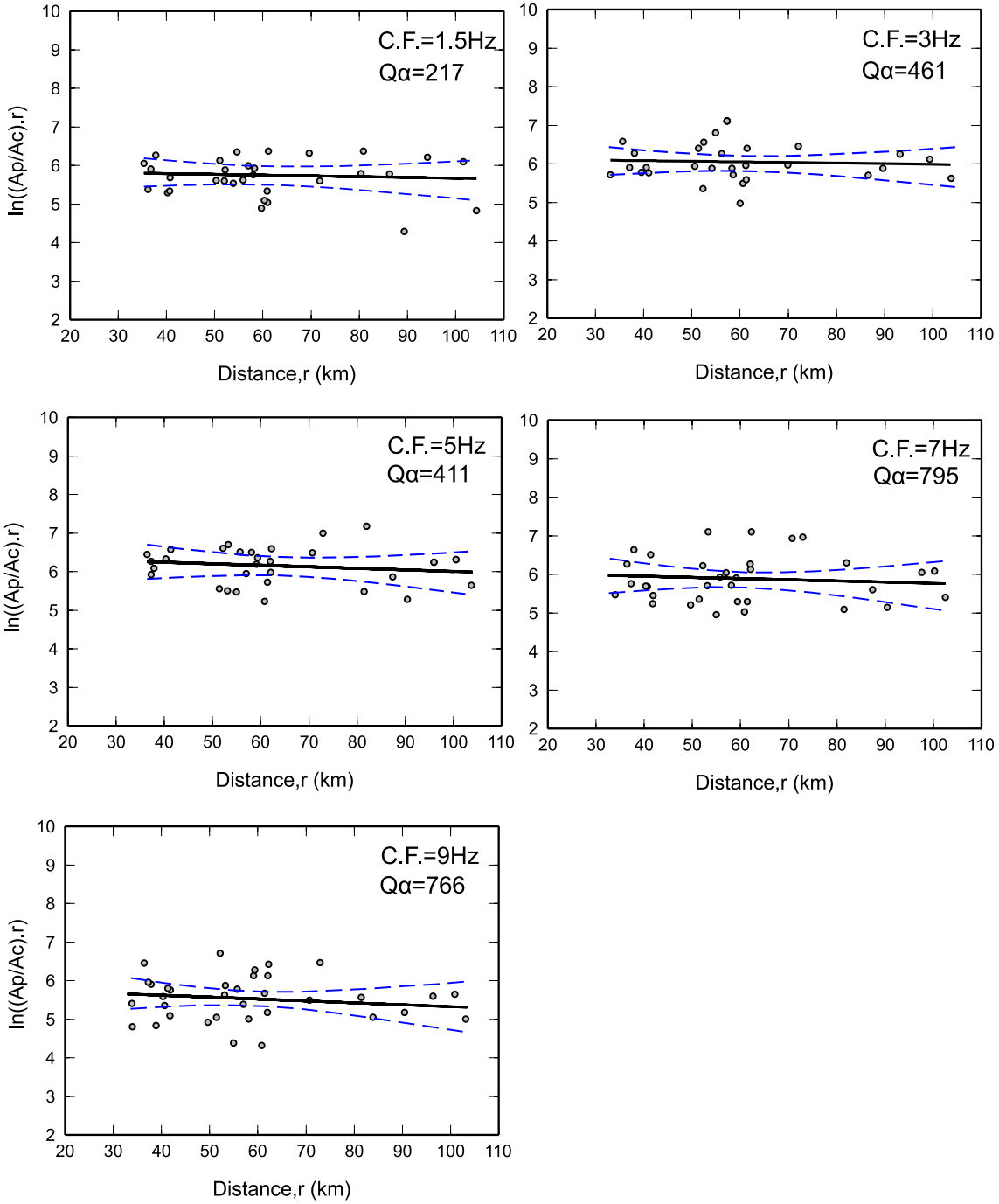

Figure 7. Plot of coda normalized peak amplitude decay of *P* waves, $\ln[(A_p/A_c)r]$ with respect to hypocentral distance r (km) at five different central frequencies for the seismic station PSK along with the least-square line drawn in solid black. Dashed lines indicate the error bound calculate at 95 per cent confidence level.

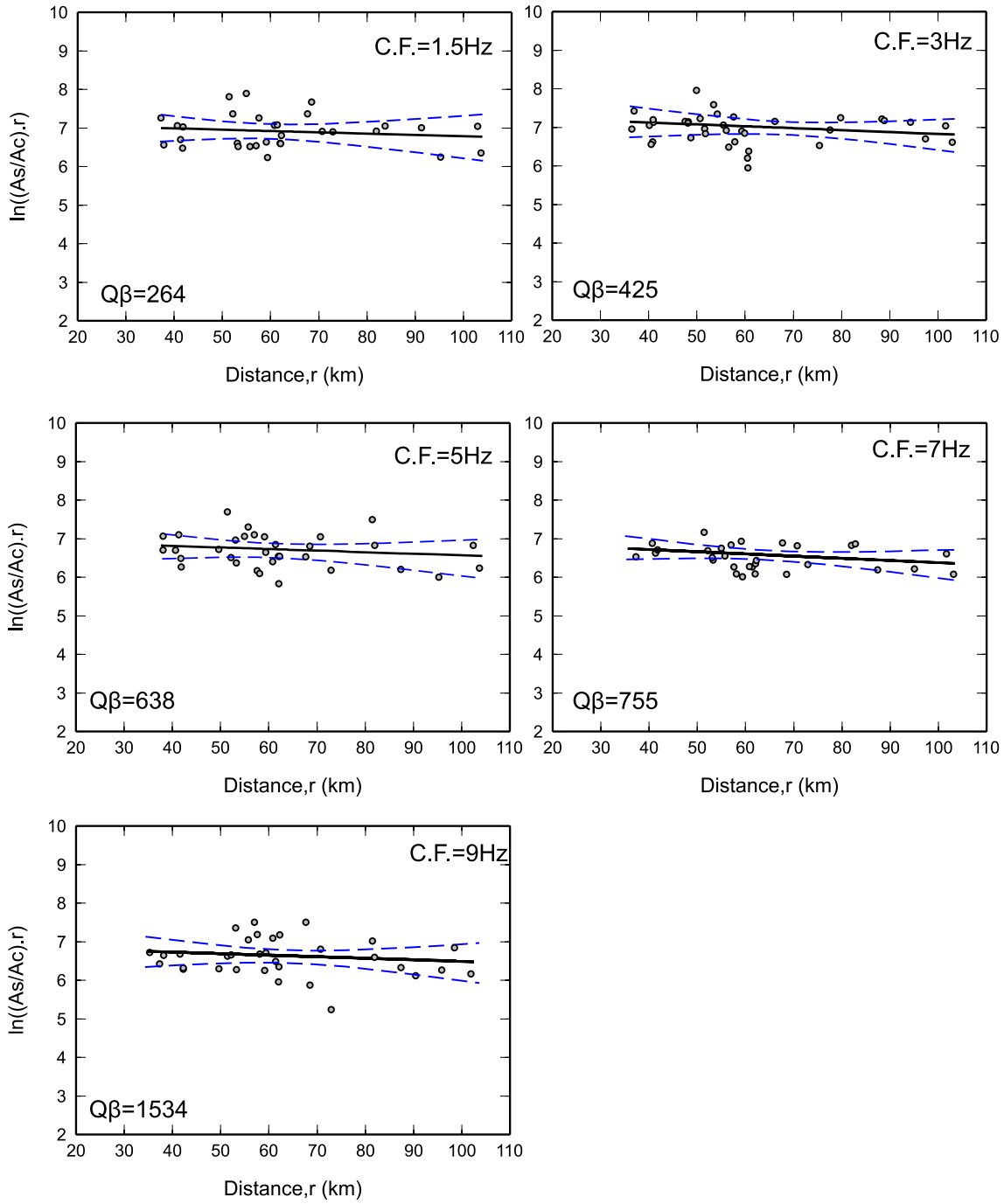

Figure 8. Plot of coda normalized peak amplitude decay of *S* waves, $\ln[(A_s/A_c)r]$ as a function of hypocentral distance r (km) at five different central frequencies for the seismic station PSK, along with the least-square line drawn in solid black. Dashed lines indicate the error bounds calculated at 95 per cent confidence level.

1984 Western Nagano prefecture, Japan earthquake. The authors also report a very weak frequency dependence of Q_β compared to Q_α and explain this discrepancy in terms of the tendency of Q_β to be constant in the crust, for high frequency seismic waves. This Q_β/Q_α value for Sikkim Himalaya is 1.04. High value of Q_β/Q_α is expected due to scattering from shallow heterogeneities in the crust (Padhy 2009). The ratio Q_β/Q_α is found to be greater than unity for the frequencies considered in this study. Earlier, a reversal of Q_β/Q_α ratio at low frequencies (<1 Hz) to high frequencies (>1 Hz) has been proposed by Yoshimoto *et al.* (1993). The ratio Q_β/Q_α is found to be larger than unity for dry rocks in the laboratory experiments (Toksoz *et al.* 1979; Mochizuki 1982; Winkler & Nur 1982). It has been reported in many studies that the ratio Q_β/Q_α is greater than unity for most of the dry and crustal rocks (e.g. Rautian *et al.* 1978; Johnston *et al.* 1979; Yoshimoto *et al.* 1993; Chung & Sato 2001). The ratio Q_β/Q_α found in the present analysis is in agreement with the laboratory experiments and the studies mentioned above.

A comparison of the estimates of Q_c ($=189f^{1.2}$) and Q_β ($=100f^{1.16}$) shows that Q_c is greater than Q_β for the frequencies

Table 5. Values of *P*-wave quality factor for different central frequencies calculated using vertical components at different seismic stations.

Station code	1.5	3	5	7	9	$Q_\alpha = Q_0 f^n$
PSK	217 ± 65	461 ± 84	411 ± 57	795 ± 95	766 ± 68	$(175 \pm 4.5)f^{(0.7 \pm 0.02)}$
GAN	205 ± 38	230 ± 83	535 ± 85	491 ± 136	556 ± 123	$(148 \pm 3.9)f^{(0.6 \pm 0.02)}$
MGN	202 ± 83	286 ± 57	709 ± 93	957 ± 195	759 ± 101	$(135 \pm 5.1)f^{(0.9 \pm 0.03)}$
MPO	246 ± 71	315 ± 97	455 ± 68	754 ± 123	1091 ± 205	$(150 \pm 3.5)f^{(0.8 \pm 0.02)}$
PHG	32 ± 13	69 ± 21	101 ± 27	458 ± 105	203 ± 89	$(18 \pm 2.9)f^{(1.3 \pm 0.1)}$
RBM	30 ± 19	370 ± 76	142 ± 74	202 ± 87	571 ± 213	$(30 \pm 13.5)f^{(1.2 \pm 0.3)}$
SIN	111 ± 43	384 ± 96	243 ± 81	558 ± 118	526 ± 120	$(98 \pm 8.3)f^{(0.8 \pm 0.08)}$
TNG	91 ± 46	211 ± 59	325 ± 96	412 ± 91	639 ± 196	$(62 \pm 0.3)f^{(1 \pm 0.01)}$

Table 6. Values of *S*-wave quality factor for different central frequencies calculated using vertical components at different seismic stations.

Station code	1.5	3	5	7	9	$Q_\beta = Q_0 f^n$
PSK	264 ± 43	425 ± 51	638 ± 102	755 ± 86	1534 ± 296	$(169 \pm 4.2)f^{(0.9 \pm 0.02)}$
GAN	221 ± 65	174 ± 42	937 ± 129	855 ± 107	912 ± 203	$(115 \pm 17.3)f^{(1 \pm 0.12)}$
MGN	257 ± 88	537 ± 67	826 ± 98	647 ± 201	954 ± 123	$(224 \pm 5.9)f^{(0.7 \pm 0.02)}$
MPO	464 ± 92	333 ± 75	721 ± 104	946 ± 141	1556 ± 235	$(250 \pm 20.1)f^{(0.7 \pm 0.07)}$
PHG	75 ± 16	149 ± 31	288 ± 73	471 ± 108	989 ± 170	$(32 \pm 1)f^{(1.4 \pm 0.02)}$
RBM	153 ± 62	457 ± 106	659 ± 174	268 ± 92	155 ± 94	$(260 \pm 90)f^{(0.1 \pm 0.2)}$
SIN	459 ± 108	655 ± 167	1124 ± 321	1245 ± 186	1093 ± 244	$(376 \pm 5.3)f^{(0.6 \pm 0.01)}$
TNG	331 ± 85	433 ± 89	576 ± 135	985 ± 234	1673 ± 339	$(195 \pm 7.6)f^{(0.9 \pm 0.03)}$

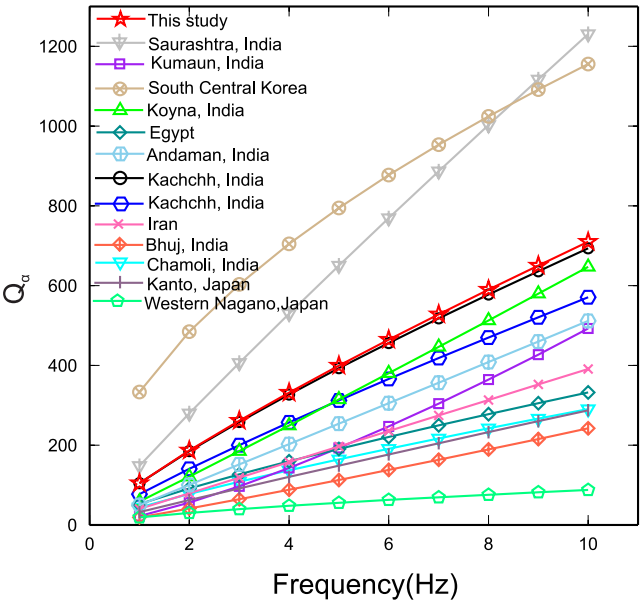

Figure 9. Comparison of estimated values of Q with those from other tectonic regions. Sources of the reported values : Saurashtra, India (Chopra *et al.* 2010); Kumaun, India (Singh *et al.* 2012); South Central Korea (Kim *et al.* 2004); Koyna, India (Sharma *et al.* 2007); Egypt (Abdel-Fattah 2009); Andaman, India (Padhy *et al.* 2011); Kachchh, India (Sharma *et al.* 2008); Kachchh, India (Chopra *et al.* 2010); Iran (Ma'hood *et al.* 2009); Bhuj, India (Padhy 2009); Chamoli, India (Mandal *et al.* 2001); Kanto, Japan (Yoshimoto *et al.* 1993); Western Nagano, Japan (Yoshimoto *et al.* 1998).

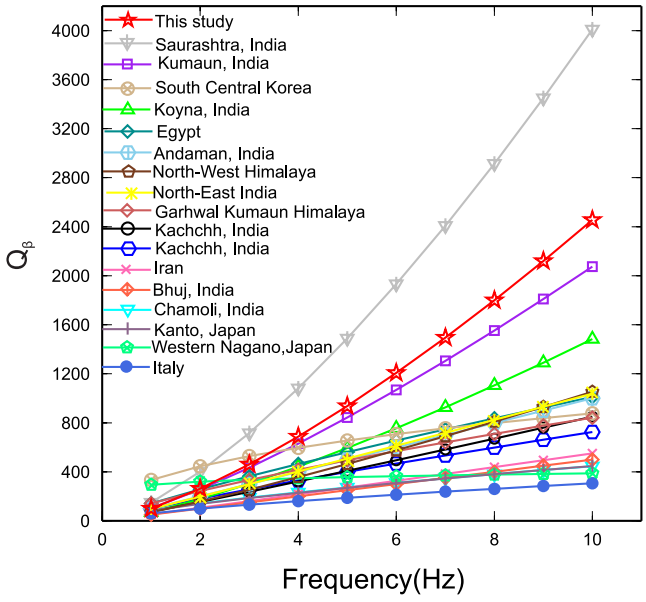

Figure 10. Comparison of the estimated values of Q and with those from other tectonic regions. Sources of the reported values are as follows: Saurashtra, India (Chopra *et al.* 2010); Kumaun, India (Singh *et al.* 2012); South Central Korea (Kim *et al.* 2004); Koyna, India (Sharma *et al.* 2007); Egypt (Abdel-Fattah 2009); Andaman, India (Padhy *et al.* 2011); North West Himalaya (Mukhopadhyay & Tyagi 2008); North-East India (Padhy & Subhadra 2010); Garhwal Kumaun Himalaya (Mukhopadhyay & Sharma 2010); Kachchh, India (Chopra *et al.* 2010); Kachchh, India (Sharma *et al.* 2008); Iran (Ma'hood *et al.* 2009); Bhuj, India (Padhy 2009); Chamoli, India (Mandal *et al.* 2001); Kanto, Japan (Yoshimoto *et al.* 1993); Western Nagano, Japan (Yoshimoto *et al.* 1998), Italy (Tuve *et al.* 2006).

considered here. It has been found by Aki (1969) and Aki & Chouet (1975) that the coda waves are dominated by *S* to *S*-backscattered waves and have a common amplitude decay (e.g. Rautian *et al.* 1978). On the other hand, Zeng *et al.* (1991) predict that the effects of intrinsic and scattering attenuation combine in a manner that Q_c should be more than Q_β. Aki (1980) observed that Q_c and Q_β are approximately equal as coda waves are backscattered *S* waves. Wennerberg (1993) explained that this observation is due to the relative weakness of scattering attenuation. The results of the present analysis support the model of Zeng *et al.* (1991). We note that this model has been found to be valid for other segments of Himalaya also (e.g. Sharma *et al.* 2009).

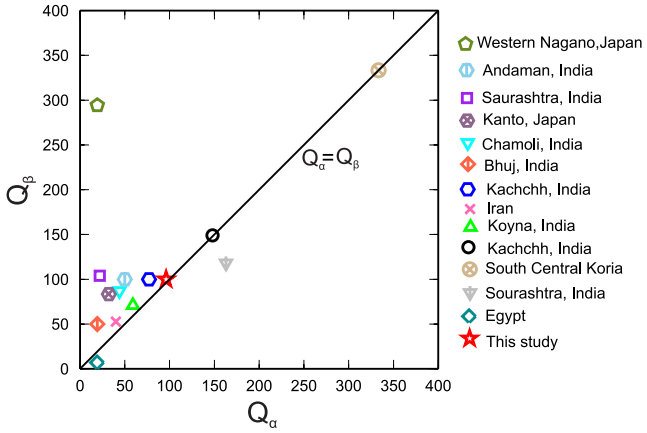

Figure 11. Comparison of Q_β / Q_α (at 1 Hz) values obtained in this study with those from other tectonic regions. Sources of the reported values: Western Nagano, Japan (Yoshimoto *et al.* 1998); Andaman, India (Padhy *et al.* 2011); Saurashtra, India (Chopra *et al.* 2010); Kanto, Japan (Yoshimoto *et al.* 1993); Chamoli, India (Mandal *et al.* 2001); Bhuj, India (Padhy 2009); Kachchh, India (Sharma *et al.* 2008); Iran (Ma'hood *et al.* 2009); Koyna, India (Sharma *et al.* 2007); Kachchh, India (Chopra *et al.* 2010); South Central Korea (Kim *et al.* 2004); Egypt (Abdel-Fattah 2009).

5.4 Determination of intrinsic (Q_i) and scattering (Q_s) attenuation

Discriminating the relative contributions of intrinsic (Q_i) and scattering (Q_s) to the total attenuation is essential to decipher the mechanism of seismic wave energy dissipation in a region. We use the approach of Wennerberg (1993) to separate Q_i and Q_s using Q_c and Q_β (eqs 8 and 9). The estimated values of Q_i and Q_s (Table 7) indicate an increase with frequency, being 228 at 1.5 Hz and 1501 at 9 Hz and the value of $Q_i < Q_s$ (Table 7). Similarly, the value of Q_s is 382 at 1.5 Hz and 4233 at 9 Hz. The relations obtained by regression analysis similar to that described earlier are $Q_i = (160 \pm 1.5)f^{(1.07 \pm 0.01)}$ and $Q_s = (298 \pm 23)f^{(1.2 \pm 0.07)}$. Also, our results indicate that the factor n is greater than unity for both intrinsic and scattering attenuation. Both values being almost similar indicates presence of heterogeneities in the study region. Fig. 12 showing the variation of Q_α, Q_β, Q_c, Q_i and Q_s with frequency reveals that Q_i is closer to Q_c and Q_s is much larger at high frequencies. This implies that the attenuation mechanism of Sikkim Himalaya is dominated by intrinsic attenuation rather than scattering attenuation, similar to that reported elsewhere (Ugalde *et al.* 2006; Sharma *et al.* 2008; Badi *et al.* 2009).

Fig. 12 shows the variation of Q_α, Q_β, Q_c, Q_i and Q_s with frequency. It has been found in theory (Frankel & Wennerberg 1987) as well as in laboratory experiments (Matsunami 1991) that Q_c is very close to Q_i. It has been revealed by Mayeda (1992), that this is valid for higher frequencies and for lower frequencies, the Q_c values are intermediate between Q_i and Q_s. The Q_c values estimated in this study lie in between Q_i and Q_s but are very close to Q_i at lower frequencies (Table 6, Fig. 12). This is in agreement with the above reported studies. A comparison between the estimated values of Q_i and Q_s shows that intrinsic absorption is predominant over scattering for the frequency range considered here.

Table 7. Average values of Q_c, Q_α, Q_β, Q_i and Q_s for five central frequencies together with the respective power laws defining frequency dependency.

C.F. (Hz)	Q_c	Q_α	Q_β	Q_i	Q_s
1.5	274	141	143	228	382
3	598	291	396	535	1524
5	1204	363	777	1068	2853
7	1475	563	962	1313	3595
9	1678	639	1108	1501	4233
$Q = Q_0 f^n$	$189f^{1.2}$	$96f^{0.94}$	$100f^{1.16}$	$160f^{1.07}$	$298f^{1.2}$

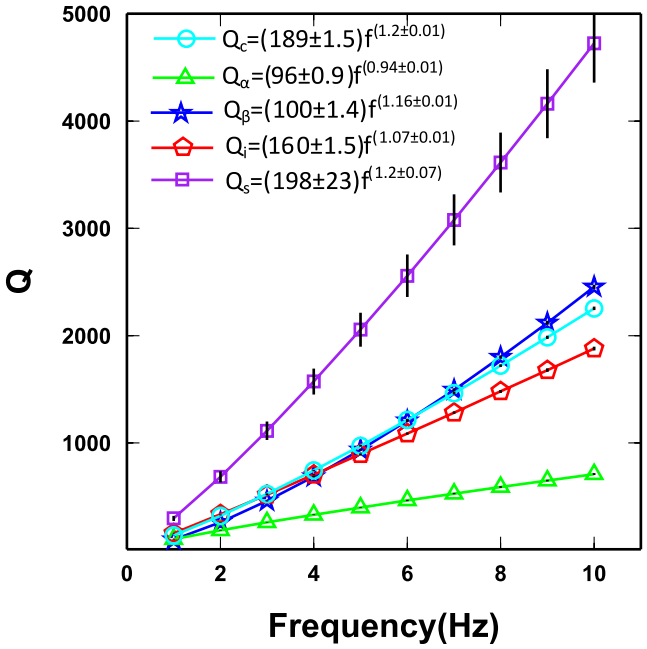

Figure 12. Plot showing the frequency dependency of Q_c, Q_α, Q_β, Q_i and Q_s values estimated in this study for Sikkim Himalaya.

6 CONCLUSIONS

The attenuation character of Sikkim Himalaya is investigated using *P*, *S* and coda waves using a total of 592 seismograms of 68 local earthquakes recorded by a seismic network operated by us. The seismic wave attenuation in this tectonic region is found to be strongly dependent on frequency. The relations that quantify this dependence for *P*, *S* and coda waves are $(96 \pm 0.9)f^{(0.94 \pm 0.01)}$, $(100 \pm 1.4)f^{(1.16 \pm 0.01)}$ and $(189 \pm 1.5)f^{(1.2 \pm 0.01)}$, respectively. The value of Q_c is found to vary both with lapse time and hypocentral depth. Also, the factor 'n' that denotes the frequency dependence is high at shallow depths but not less than unity, and the value of Q_0 increases with depth. These observations favour a heterogeneous crust. A comparison of the attenuation parameters obtained in this study with those from other tectonic regions reveals slightly higher Q values for the Sikkim Himalaya, in conformity with the moderate seismicity that this region experiences relative to the other segments of Himalaya. The ratio between Q_β and Q_α is found to be 1.04, similar to global findings. Further, the intrinsic and scattering attenuation values also reveal a frequency dependence that can be expressed as $Q_i = (160 \pm 1.5)f^{(1.07 \pm 0.01)}$ and $Q_s = (298 \pm 23)f^{(1.2 \pm 0.07)}$. The results imply that the mechanism of seismic wave attenuation in Sikkim Himalaya is dominated by intrinsic rather than scattering attenuation. The estimated Q_c values are found to be higher than Q_β for Sikkim Himalaya, consistent with the model of Zeng *et al.* (1991) which predicts that the effects of intrinsic and scattering attenuation combine in a manner that Q_c should be more than Q_β.

ACKNOWLEDGEMENTS

The work is supported by a project on eastern Himalaya supported by the Ministry of Earth Sciences. Part of the work has been performed under the GENIAS project of CSIR-NGRI. We sincerely thank two anonymous reviewers for their extremely useful comments. We thank CSIR for the Senior Research Fellowship to Pinki Hazarika.

REFERENCES

Abdel-Fattah, A.K., 2009. Attenuation of body waves in the crust beneath the vicinity of Cairo Metropolitan area (Egypt) using coda normalization method, *Geophys. J. Int.,* **176,** 126–134.

Aki, K., 1969. Analysis of the seismic coda of local earthquakes as scattered waves, *J. geophys. Res.,* **74,** 615–631.

Aki, K., 1980. Attenuation of shear waves in the lithosphere for frequencies from 0.05 to 25 Hz, *Phys. Earth planet. Inter.,* **21,** 50–60.

Aki, K., 1981. Source and scattering effects on the spectra of small local earthquakes, *Bull. seism. Soc. Am.,* **71,** 1687–1700.

Aki, K. & Chouet, B., 1975. Origin of the coda waves: source, attenuation, and scattering effects, *J. geophys. Res.,* **80,** 3322–3342.

Akinci, A., Taktak, A.G. & Ergintav, S., 1994. Attenuation of coda waves in Western Anatolia, *Phys. Earth planet. Inter.,* **87,** 155–165.

Badi, G., Del Pezzo, E., Ibanez, J.M., Bianco, F., Sabbione, N. & Araujo, M., 2009. Depth dependent seismic scattering attenuation in the Nuevo Cuyo region (southern central Andes), *Geophys. Res. Lett.,* **36,** L24307, doi:10.1029/2009GL041081.

Chopra, S., Kumar, D. & Rastogi, B.K., 2010. Attenuation of high frequency *P* and *S* waves in the Gujarat region, India, *Pure. appl. Geophys.,* **168,** 797–813.

Chung, T.W. & Lee, K., 2003. A study of high-frequency Q_{Lg}^{-1} in the crust of South Korea, *Bull. seism. Soc. Am.,* **93,** 1401–1406.

Chung, T.W. & Sato, H., 2001. Attenuation of high frequency *P* and *S* waves in the crust of southeastern South Korea, *Bull. seism. Soc. Am.,* **91,** 1867–1874.

De, R. & Kayal, J.R., 2004. Seismic activity at the MCT in Sikkim Himalaya, *Tectonophysics,* **386,** 243–248.

Frankel, A. & Wennerberg, L., 1987. Energy-flux model for seismicoda: separation of scattering and intrinsic attenuation, *Bull. seism. Soc. Am.,* **77,** 1223–1251.

Geological Survey of India, 2000. *Seismotectonic Atlas of India and its Environs,* GSI, p. 87.

Giampiccolo, E., Tusa, G., Langer, H. & Gresta, S., 2002. Attenuation in southeastern Sicily (Italy) by applying different coda methods, *J. Seismol.,* **6,** 487–501.

Gupta, A.K., Sutar, A.K., Chopra, S., Kumar, S. & Rastogi, B.K., 2012. Attenuation characteristic of coda waves in Mainland Gujarat (India), *Tectonophysics,* **530–531,** 264–271.

Gupta, S.C., Teotia, S.S., Rai, S.S. & Gautam, N., 1998. Coda Q estimates in the Koyna region, India, *Pure. appl. Geophys.,* **153,** 713–731.

Havskov, J. & Ottemller, L., 2005. *SEISAN: The Earthquake Analysis Software, Version 8.0,* Institute of Solid Earth Physics, University of Bergen, Bergen, Norway.

Hazarika, P., Kumar, M.R., Srijayanthi, G., Raju, P.S., Rao, N.P. & Srinagesh, D., 2010. Transverse tectonics in Sikkim Himalaya: evidences from seismicity and focal mechanism data, *Bull. seism. Soc. Am.,* **100,** 1816–1822.

Ibanez, J.M., del Pezzo, E., de Miguel, F., Herraiz, M., Alguagh, G. & Morales, J., 1990. Depth dependent seismic attenuation in the Granada zone (southern Spain), *Bull. seism. Soc. Am.,* **80,** 1222–1234.

IS 1893 (Part 1), 2002. *Indian Standard Criteria for Earthquake Resistant Design of Structures,* 5th Rev., Bureau of Indian Standards, New Delhi. Available at: http://www.mausam.gov.in/WEBIMD/seismic_zone_map.jsp. Last accessed April 2012.

Johnston, D.H., Toksoz, M.N. & Timur, A., 1979. Attenuation of seismic waves in dry and saturated rocks: I. Mechanics, *Geophysics,* **44,** 691–711.

Kayal, J.R., 2001. Microearthquake activity in some parts of the Himalaya and tectonic model, *Tectonophysics,* **339,** 331–351.

Kim, K.D., Chung, T.W. & Kyung, J.B., 2004. Attenuation of high-frequency P and S waves in the crust of Choongchung provinces, Central South Korea, *Bull. seism. Soc. Am.,* **94,** 1070–1078.

Knopoff, L., 1964. Q, *Rev. Geophys.,* **2,** 625–660.

Kvamme, L.B. & Havskov, J., 1989. Q in Southern Norway, *Bull. seism. Soc. Am.,* **79,** 1575–1588.

Leary, P.C., 1995. The cause of frequency-dependent seismic absorption in crustal rock, *Geophys. J. Int.,* **122,** 143–151.

Lay, T. & Wallace, T.C., 1995. *Modern Global Seismology,* Academic Press, p. 113.

Ma'hood, M., Hamzehloo, H. & Doloei, G.J., 2009. Attenuation of high frequency P and S waves in the crust of the East-Central Iran, *Geophys. J. Int.,* **179,** 1669–1678.

Matsunami, K., 1991. Laboratory tests of excitation and attenuation of coda waves using 2-D models of scattering media, *Phys. Earth planet. Inter.,* **67,** 36–47.

Matsunami, K. & Nakamura, M., 2004. Seismic attenuation in a nonvolcanic swarm region beneath Wakayama, southwest Japan, *J. geophys. Res.,* **109,** B09302, doi:10.1029/2003JB002758.

Mayeda, K., Koynagi, S., Hoshiba, M., Aki, K. & Zeng, Y., 1992. A comparative study of scattering, intrinsic and coda Q for Hawaii, Long Valley, and Central California between 1. 5 and 15 Hz, *J. geophys. Res.,* **97,** 6643–6659.

Mitchell, B.J., 1981. Regional variation and frequency dependence of Q in the crust of the United States, *Bull. seism. Soc. Am.,* **71,** 1531–1538.

Mochizuki, S., 1982. Attenuation in partially saturated rocks, *J. geophys. Res.,* **87,** 8598–8604

Mukhopadhyay, S. & Sharma, J., 2010. Attenuation characteristics of Garwhal-Kumaun Himalayas from analysis of coda of local earthquakes, *J. Seismol.,* **14,** 693–713.

Mukhopadhyay, S., Sharma, J., Massey, R. & Kayal, J.R., 2008. Lapse time dependence of coda Q in the source region of the 1999 Chamoli earthquake, *Bull. seism. Soc. Am.,* **98,** 2080–2086.

Mukhopadhyay, S., Sharma, J., Del-Pezzo, E. & Kumar, N., 2010. Study of attenuation mechanism for Garwhal-Kumaun Himalayas from analysis of coda of local earthquakes, *Phys. Earth planet. Inter.,* **180,** 7–15.

Padhy, S., 2009. Characteristics of body wave attenuations in the Bhuj crust, *Bull. seism. Soc. Am.,* **99,** 3300–3313.

Padhy, S. & Subhadra, N., 2010. Attenuation of high-frequency seismic waves in northeast India, *Geophys. J. Int.,* **181,** 453–467.

Padhy, S., Subhadra, N. & Kayal, J. R., 2011. Frequency-dependent attenuation of body and coda waves in the Andaman Sea Basin, *Bull. seism. Soc. Am.,* **101,** 109–125.

Paul, A., Gupta, S.C. & Pant, C., 2003. Coda Q estimates for Kumaun Himalaya. *Proc. Indian Acad. Sci. (Earth Planet. Sci.)*., **112,** 569–576.

Rautian, T.G. & Khalturin, V.I., 1978. The use of coda for the determination of the earthquake source spectrum, *Bull. seism. Soc. Am.,* **68,** 923–948.

Roecker, S.W., Tucker, B., King, J. & Hartzfield, D., 1982. Estimates of Q in Central Asia as a function of frequency and depth using the coda of locally recorded earthquakes, *Bull. seism. Soc. Am.,* **72,** 129–149.

Sato, H., 1977. Energy propagation including scattering effect: single isotropic scattering approximation, *J. Phys. Earth,* **25,** 27–41.

Sato, H., 1984. Attenuation of envelope formation of three component seismograms of small local earthquakes in randomly inhomogeneous lithosphere, *J. geophys. Res.,* **89,** 1221–1241.

Sato, H. & Fehler, M.C., 1998. *Seismic Wave Propagation and Scattering in the Heterogeneous Earth,* Springer-Verlag, New York.

Savage, J.C., 1965. Attenuation of elastic waves in granular medium, *J. geophys. Res.,* **70,** 3935–3943.

Savage, J.C., 1966. Thermoelastic attenuation of elastic waves by cracks, *J. geophys. Res.,* **71,** 3929–3938.

Sharma, B., Teotia, S.S. & Kumar, D., 2007. Attenuation of P, S, and coda waves in Koyna region, India, *J. Seismol.,* **11,** 327–334.

Sharma, B., Gupta, A.K., Devi, D.K., Kumar, D., Teotia, S.S. & Rastogi, B.K., 2008. Attenuation of high frequency seismic waves in Kachchh region, Gujarat, India, *Bull. seism. Soc. Am.,* **98,** 2325–2340.

Sharma, B., Teotia, S.S., Kumar, D. & Raju, P.S., 2009. Attenuation of P- and S-waves in the Chamoli Region, Himalaya, India, *Pure. appl. Geophys.,* **166,** 1949–1966.

Singh, C., Singh, A., Srinivasa Bharathi, V.K., Bansal, A.R. & Chadha, R.K, 2012. Frequency-dependent body wave attenuation characteristics in the Kumaun Himalaya, *Tectonophysics,* **524–525,** 37–42.

Toksoz, M.N., Johnston, A.H. & Timur, A., 1979. Attenuation of seismic waves in dry and saturated rocks I. Laboratory measurements, *Geophysics,* **44,** 681–690.

Tsujiura, M., 1978. Spectral analysis of the coda waves from local earthquakes, *Bull. earthq. Res. Inst. Univ. Tokyo,* **53,** 1–48.

Tuve, T., Bianco, F., Ibez, J., Patan, D., Del Pezzo, E. & Bottari, A., 2006. Attenuation study in the Straits of Messina area (southern Italy), *Tectonophysics,* **421,** 173–185.

Ugalde, A., Tripathi, J.N., Hoshiba, M. & Rastogi, B.K., 2006. Intrinsic and scattering attenuation in western India from aftershocks of the 26 January, Kachchh earthquake, *Tectonophysics,* **429,** 111–123.

Waldhauser, F., 2001. HypoDDA program to compute double-difference hypocenter locations, U.S. Geol. Surv. Open-File Report, 01-113, pp.113.

Wennerberg, L., 1993. Multiple-scattering interpretation of coda-Q measurements, *Bull. seism. Soc. Am.,* **83,** 279–290.

Winkler, K.W. & Nur, A., 1982. Seismic attenuation effects of pore fluids and frictional sliding, *Geophysics,* **47,** 1–15.

Wu, R., 1985. Multiple scattering and energy transfer of seismic waves: separation of scattering effect from intrinsic attenuation: I. Theoretical modeling, *Geophys. J. R. astr. Soc.,* **82,** 57–80.

Yoshimoto, K., Sato, H. & Ohtake, M., 1993. Frequency-dependent attenuation of *P* and *S* waves in the Kanto area, Japan, based on the coda normalization method, *Geophys. J. Int.,* **114,** 165–174.

Yoshimoto, K., Sato, H., Ito, Y., Ito, H., Ohminato, T. & Ohtake, M., 1998. Frequency dependent attenuation of high-frequency *P* and *S* waves in the upper crust in western Nagano, Japan, *Pure. appl. Geophys.,* **153,** 489–502.

Zener, C., 1948. *Elasticity and Anelasticity of Metals,* University of Chicago Press, Chicago, I11.

Zeng, Y., Su, F. & Aki, K., 1991. Scattered wave energy propagation in a random isotropic scattering medium, I, theory, *J. geophys. Res.,* **96,** 607–619.